Study of Active Galactic Nuclei using the Water Vapour Masers

Deepshikha[1], *Nakai Naomasa*[2], *Yamazaki Madoka*[3], *Yamauchi Aya*[4]

Graduate School of Science and Technology, Kwansei Gakuin University[1,2], *Degree Program in Education, University of Tsukuba*[3], *Mizusawa VLBI Observatory, National Astronomical Observatory of Japan*[4]

The mass of the black hole separated from the mass of the maser disk is calculated using the mega-maser technique for 15 maser-galaxies and the corresponding Magorrian relationship ($M_{BH} - \sigma$) is analysed.

Introduction

In the surroundings of some Active Galactic Nuclei (AGN), the hot (500K) dense molecular gas (10^{7-10}cm^{-3})that probes the region closer to the central engine i.e. a black hole (BH), radiates extremely luminous mega-maser emission. They have a characteristic spectral profile usually with two distinct groups: one centred near the systemic recession velocity (V_{sys}) of the galaxy while the other includes the high-velocity features, blue-shifted or red-shifted, whose Very Long Baseline Interferometry (VLBI) observations are used to plot the rotational velocity (V_{rot}) curves.

Data

Velocities, distances to the AGNs (Mpc), right ascension and declination values (mas) of the systemic and high-velocity features were taken from literatures (Mamyoda et al. 2009; Kondratko et al. 2008; Kuo et al. 2011; Gao et al. 2017, 2017; Zhao et al. 2018), the BH masses of non-maser galaxies and the velocity dispersion values of the bulges from Sahu et al. (2019). The angular resolution was 1 mas or less.

Methods

Using the VLBI images of the distribution of maser spots, the position angles of the mega-maser disks are calculated assuming the disks to be edge-on and the rotation curves are plotted using $V_{rot} = V_{LSR} - V_{sys}$, where V_{LSR} is the line-of-sight velocity with respect to the Local Standard of Reference. Since the sub-parsec disks used for analysis are in gravitational potentials near the BH, special and general relativistic corrections are done in the data to increase the accuracy (although the effects are minimal). Moreover, in order to see if the disk is following the Keplerian rotation or not, a position-velocity relationship, equation (1) is fitted with α as one of the free parameters. If $|\alpha| = 0.5$, the orbit is Keplerian (point mass, BH) whereas if $|\alpha| < 0.5$, it is Non-Keplerian (extended/non-negligible mass, BH+maser disk)

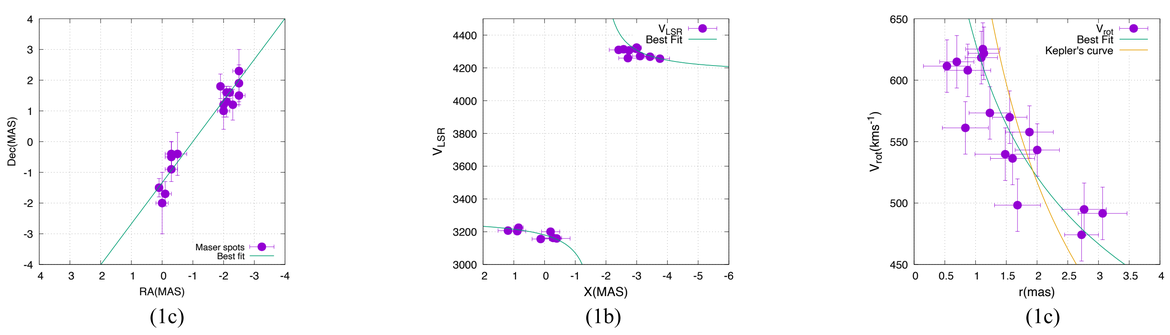

Figure 1: (1a) Distribution of maser spots , (1b) Plot for line-of-sight velocities for blue-shifted and red-shifted maser features of NGC3393 (as an example), and (1c) Keplerian and Non-Keplerian rotation curves for NGC3393

$$V_{LSR} = A(X - X_0)^{\alpha} + V_{sys} \tag{1}$$

where A and α are constants, X is a coordinate along the edge-on disk, and X_0 is the position of BH.

Mass Model

The Non-Keplerian rotation indicates that the mass causing the gravitational field is not reducible to a point but is extended. The maser disk is assumed to be in a plane that contains the accretion disk and an outer gaseous disk surrounding the fixed BH (Hure 2002). To calculate M_{BH}, a position-velocity curve is fitted using the equation (2) (Hure 2002; Hure et. al 2007, 2008; Mamyoda et. al 2009) where the disk is assumed to be a Mestel disk.

$$V_{rot} = |V_{LSR} - V_{sys}| = \sqrt{\frac{GM_{BH}}{X - X_0} + 2\pi G\Sigma_0 a_{out}} \tag{2}$$

where a_{out} is the outer edge of the gaseous disk and Σ_{out} is the surface density of the gas at a_{out}.

Velocity Correction

1. Gravitational Shift (General Relativity)

For an i^{th} maser in a circular orbit moving at a speed $\beta_{m_i}c$ (β_m is the beta factor for maser), the gravitational acceleration is balanced by the centripital acceleration (Kuo et al. 2011),

$$\frac{GM}{r^2} = \frac{(\beta_{m_i}c)^2}{r} \tag{3}$$

$$z_i = \frac{1}{c}\left(\frac{v_{rot_i}}{1+\beta_m^2}\right) \tag{4}$$

2. Doppler's Shift (Special Relativity)

$$V_{true_i} = \pm c\left(\frac{(1+z_i)^2 - 1}{(1+z_i)^2 + 1}\right) \tag{5}$$

Results

Table 1. Results

AGN	$\lvert\alpha\rvert$	$M_{BH}(10^6 M_0)$	$M_{disk}(10^6 M_0)$	*D(Mpc)*
ES0558-G009	0.362 ± 0.022	13.05 ± 0.80	3.09 ± 0.91	111.25 ± 0.59
J0437+2456	0.303 ± 0.037	1.85 ± 0.23	0.82 ± 0.26	68.27 ± 0.45
Mrk1029	0.310 ± 0.065	0.57 ± 0.16	0.93 ± 0.65	126.787 ± 0.059
NGC1194	0.407 ± 0.004	59.81 ± 0.66	9.41 ± 0.37	55.31 ± 0.4
NGC1320	0.479 ± 0.078	4.71 ± 0.58	0.10 ± 1.14	38.4 ± 0.44
NGC2273	0.322 ± 0.043	5.93 ± 0.75	1.87 ± 0.85	25.2 ± 0.25
NGC2960	0.467 ± 0.020	12.14 ± 0.46	1.02 ± 0.89	75.61 ± 0.38
NGC3393	0.273 ± 0.055	12.09 ± 3.15	29.60 ± 7.77	58.41 ± 0.3
NGC4388	0.389 ± 0.052	16.07 ± 1.77	0.74 ± 7.22	41.41 ± 0.66
NGC5495	0.371 ± 0.035	6.51 ± 3.47	2.45 ± 3.30	100.84 ± 0.66
NGC5765b	0.519 ± 0.006	49.70 ± 0.55	-2.22 ± 0.65	126 ± 11
NGC6264	0.477 ± 0.009	28.71 ± 0.55	2.13 ± 1.00	137 ± 19
NGC6323	0.520 ± 0.013	10.44 ± 0.27	-0.47 ± 0.25	107 ± 42
UGC3789	0.548 ± 0.011	10.98 ± 0.22	-1.25 ± 0.31	45 ± 4.7
UGC6093	0.498 ± 0.083	26.96 ± 3.27	0.68 ±6.45	161.2 ± 0.96

Figure 2 shows the Maggorian Relationship due to the proper motion [P], stellar dynamical modelling [S], gas dynamical modelling [G], stellar gas dynamical modelling [SG], direct imaging [DI] and mega-maser technique of disk-mass model The masses calculated by the mega-maser technique using the existing maser data (Gao et. al 2017; Kuo et. al 2011; Kondratko et. al 2008; Gao et. al 2016; Zhao et. al 2018) are plotted in the $M_{BH} - \sigma$ plot (σ is the velocity dispersion of the stars in the bulge of the galaxy) but they are not included in the linear fit, showing that these are usually lighter than those calculated using other techniques.

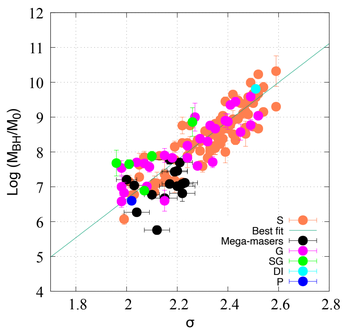

Figure 2

Conclusion

1. The orbits were checked to see whether they are Keplerian or not and if the mass distribution is pointed or extended.
2. M_{BH} separated from the M_{disk} was calculated while adapting the disk-mass model using the existing maser data of 15 mega-maser galaxies assuming the disk to be Mestel.
3. $M_{BH} - \sigma$ relationship was plotted using the data from Nandini et. al (2019) that includes the non-maser techniques. The calculated masses were plotted in the same graph for comparison. It may be concluded that since maser discs are extremely close to the central engines and cover lesser radii, this technique gives more precise M_{BH} separated from the M_{disk}. Hence, most of the M_{BH} of mega-maser galaxies are much lower than the mass expected by the $M_{BH} - \sigma$ relationship of the non-maser techniques.

References

1. Gao, F., Braatz, J., A., Reid, M., J., Lo, K., Y., Condon, J., J., Henkel, C., Kuo, C., Y., Impellizzeri, C., M., V., Pesce, D., W., Zhao, W. 2016, ApJ, 817, 128
2. Gao, F., Braatz, J., A., Reid, M.,J., Condon, J., J., Greene, J., E., Henkel, C., Impellizzeri, C., M., V., Lo, K., Y., Kuo, C., Y., Pesce, D., W. 2017, ApJ, 834, 52
3. Hur´e, J.,-M., 2002, A&A, 395, L21
4. Hur´e, J.,-M., & Hersant, F. 2007, A&A, 467, 907
5. Hur´e, J.,-M., Hersant, F., Carreau, C., Busset, J., -P. 2008, A&A, 490, 477
6. Kondratko, P., T., Greenhill, L., J., Moran, J., M. 2008, ApJ, 678, 87
7. Kuo, C. Y., Braatz, J., A., Condon, J., J., Impellizzeri, C., M., V., Lo, K., Y., Zaw, I., Schenker, M., Henkel, C., Reid, M., J., Greene, J., E. 2011, ApJ, 727, 20
8. Mamyoda, K., Nakai, N., Yamauchi, A., Diamond, P., Hur´e, J., -M. 2009, PASJ, 61, 1143
9. Nandini, S., Alister, W., G., Benjamin, L., D. 2019, ApJ, 887, 10
10. Reid, M., J., Braatz, J., A., Condon, J., J., Greenhill, L., J., Henkel, C., Lo, K., Y. 2009, ApJ, 695, 287
11. Zhao, W., Braatz, J., A., Condon, J., J., Lo, K., Y., Reid, M., J., Henkel, C., Pesce, D., W., Greene, J., E., Gao, F., Kuo, C., Y. 2018, ApJ, 854, 124Z